Effect of Enhanced Convection on the Microstructure of Al-Cu-Li Welds

Microstructural analysis of welds made at different gravity levels reveal changes in the narrow band of fine equiaxed grains along the fusion zone

BY D. K. AIDUN AND J. P. DEAN

ABSTRACT. The effects of enhanced convection induced by a high-gravity environment on the resulting weld microstructure of a 2195-T8 (Al-Cu-Li) alloy have been investigated. Stationary (spot) bead-on-plate gas tungsten arc welds were performed at 1, 5 and 10 g (1 g = 9.8 m/s^2) using the multigravity research welding system (MGRWS). Of particular interest was the gradual disappearance of a narrow band of fine equiaxed grains (EQ) located along the fusion boundary of the weld as g level increased. The presence of this equiaxed zone (EQZ) may affect weld mechanical properties and therefore compromise structures incorporating welds of Al-Cu-Li alloys.

The qualitative verification of a proposed mechanism for equiaxed grain formation along the fusion boundary of Al-Cu-Li alloy welds by Gutierrez and Lippold is also presented. This mechanism proposes that EQZ formation occurs by heterogeneous nucleation aided by Al_3Zr and Al_3(Li, Zr) precipitates in a stagnant boundary layer located in the unmixed zone of the fusion boundary layer. Here, thermal and fluid flow conditions are believed to be insufficient to sweep the precipitates into the weld pool, hence causing the formation of the EQZ.

The high-g environment causing enhanced convection is believed to alter the thermal and fluid flow conditions within the weld pool, thereby creating an environment in which there is neither a stagnant boundary layer nor an unmixed zone. Furthermore, the precipitates aiding in the precipitation of the fine, equiaxed grains are believed to be swept into the weld pool at high-g and completely dissolved. As a result, the environment for equiaxed grain formation has been eliminated. The analysis of the microstructural evolution from 1 to 5 to 10 g qualitatively verifies this proposed mechanism. At 1 g, a prominent EQZ formed; at 5 g, the EQZ was scattered in location along the fusion boundary and of reduced width; at 10 g, the EQZ had completely disappeared leaving a near perfect line separating the large grains of the heat-affected zone from the fine dendrites of the fusion zone.

D. K. AIDUN and J. P. DEAN are with Clarkson University, Potsdam, N.Y.

Introduction

Aluminum-lithium alloys represent an advanced development in high-performance, weight-saving aluminum alloys designed for aerospace, including, most recently, cryogenic applications for liquid hydrogen and liquid oxygen fuel tanks for launch vehicles. Promising features of aluminum-lithium alloys include advantages in strength and stiffness over conventional 2XXX- and 7XXX- series aluminum alloys. Major development of aluminum-lithium alloys began in the 1970s in an effort to introduce lower-density and higher-performance aluminum alloys into aircraft structural components. This development led to the introduction of 8090, 2090 and 2091 commercial alloys in the 1980s, with the Weldalite 049 family the most recent development in aluminum-lithium technology (Refs. 1, 2).

To take advantage of these promising features in structural applications, methods of joining aluminum-lithium, particularly welding, must be thoroughly investigated and understood to maximize the structural capabilities of this light alloy. The Weldalite 049 family represents a favorable alternative to both conventional aluminum alloys and other aluminum-lithium alloys used in welded structures because of its good weldability, greater yield strengths and improved fracture toughness (Ref. 2). However, relatively little research has been performed on microstructural characterization and mechanical properties of welded aluminum-lithium alloys, including the Weldalite 049 family, when compared to the level of research conducted on as-quenched and various heat-treated Al-Li and Al-Li-X alloys. This is particularly true with regards to novel welding processes, namely multigravity gas tungsten arc (GTA) welds, which attempts to eliminate weld defects through enhanced convection flow by means of inducing a high-gravity environment on weld geometry and solidification structure. The development and implementation of novel welding processes, such as a multigravity welding process, may lead to the use of Weldalite 049 and other aluminum-lithium alloys in light armored vehicles, marine hardware and extensive space applications for small-size structures and components (Refs. 1, 3).

KEY WORDS

Al-Cu-Li Alloys
Weldalite
GTAW
Gravity
Aerospace
Cryogenic
Gas Tungsten Arc
HAZ

This paper discusses the qualitative verification of a proposed mechanism for equiaxed grain (EQ) formation along the fusion boundary of Al-Cu-Li welds proposed by Gutierrez and Lippold (Ref. 4). The findings of a microstructural characterization of multigravity spot GTA welds of 2195-T8 alloy will be discussed. The effects of enhanced buoyancy force on weld geometry, varying microstructure and orientation within the fusion and heat-affected zones and the gradual disappearance of an equiaxed band of fine grains located along the fusion boundary with increasing g-level will be addressed.

Background

Since the 1970s, a growing and significant interest in aluminum-lithium alloys has occurred. This is primarily due to lithium's unique ability to decrease the

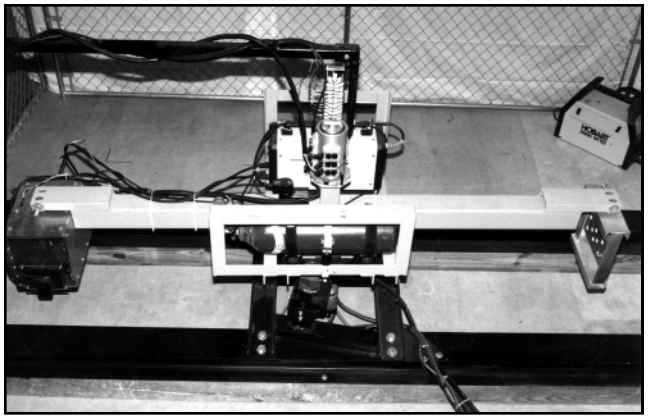

Fig. 1 — Multigravity research welding system (MGRWS).

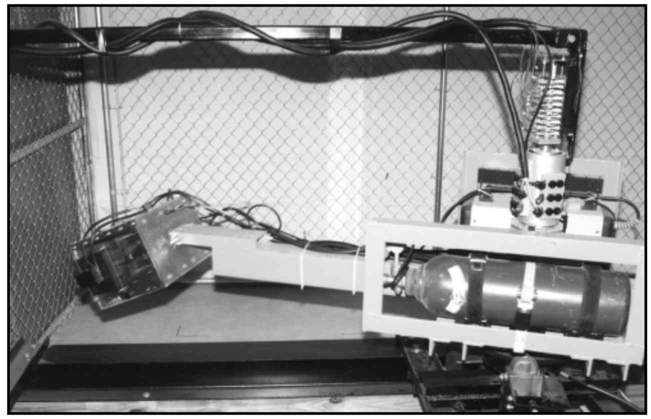

Fig. 2 — MGRWS during rotation.

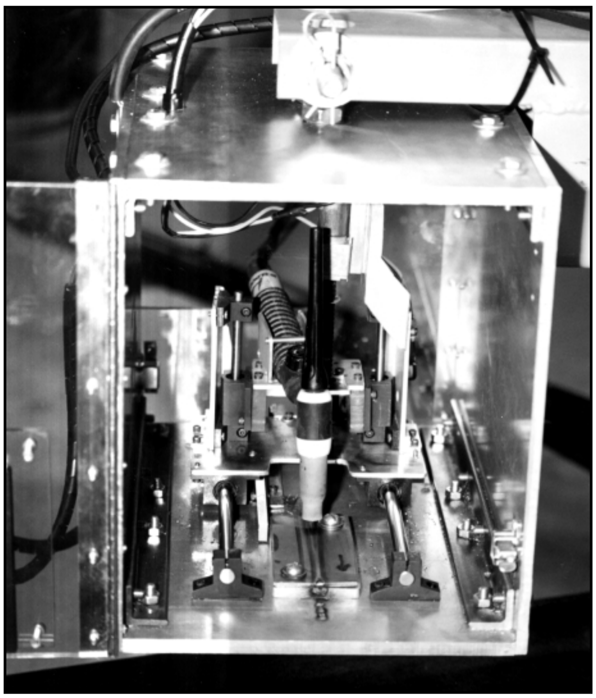

Fig. 3 — Welding box.

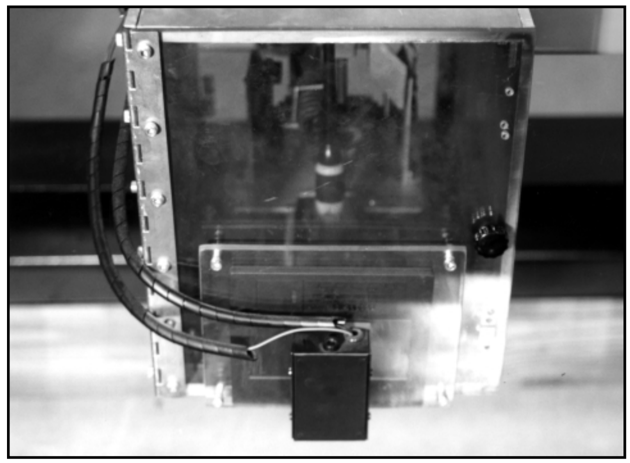

Fig. 4 — View of the camera attached to the door of the welding box.

density and increase the stiffness characteristics of aluminum alloys of comparable strength. Lithium is the lightest metallic element, and each 1 wt-% of lithium (up to the 4.2% Li solubility limit) reduces alloy density by about 3% and increases modulus by about 5% (Refs. 1, 5, 6).

The strengthening mechanism in Al-Li alloys involves the continuous precipitation of δ′ (Al_3Li) phase from a supersaturated solution. The composition of the δ′ precipitates consists of eight shared corner sites occupied by lithium and six shared faces occupied by aluminum. Geometric similarity between the lattice of the precipitates and the face-centered cubic lattice of the solid solution facilitates the observed cube/cube orientation dependence (Refs. 1, 7–9). Once the major strengthening precipitate δ′ is homogeneously precipitated, it remains coherent after extensive aging with particle size distributions (PSD) of δ′ to be a function of alloy composition and considered to be a steady-state distribution. In addition, the coefficient of variation increases with increasing lithium content, *i.e.,* as lithium content increases, the PSD broadens (Ref. 10).

Despite the precipitation-strengthening mechanism of δ′, the low ductility and toughness of binary aluminum-lithium alloys is caused by, in some part, the inhomogeneous nature of their slip. This is due to coherent-particle hardening of the δ′ precipitate. In addition to the coarsening of δ′ during aging, a grain boundary reaction involving the growth of equilibrium δ (AlLi) phase occurs. The solute required to supply this growth is provided by dissolution of δ′ in the vicinity of grain boundaries. This results in a particle-free zone (PFZ), which grows parabolically with time at the very early stages of aging and continues through the aging process until all of δ′ is consumed. The presence of these PFZs can then induce strain localization and promote intergranular failure (Refs. 10, 11).

To realize the possible benefits of these alloys, joining techniques, particularly welding, must be investigated and understood in order to maximize applications incorporating aluminum-lithium components. One of the most promising aluminum-lithium alloys for welded aerospace applications is the Weldalite 049 family of alloys (2094, 2095 and 2195) designed and developed by Martin Marietta Laboratories. Alloy 2195 is the leading alloy and is designed to replace alloys 2219 and 2014 for launch applications. Primary launch applications include propellant tankage, which constitutes the bulk of the dry weight of space launch systems (Ref. 2). Cryogenic properties are an important factor in the overall com-

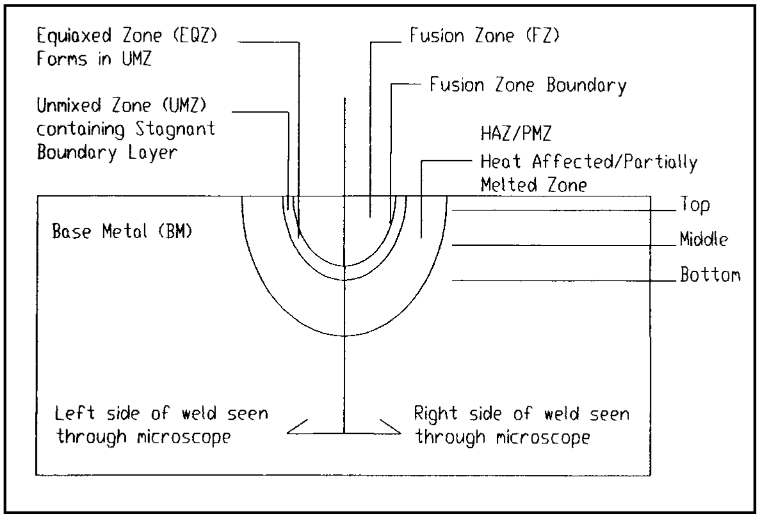

Fig. 5 — Nomenclature for various weld regions.

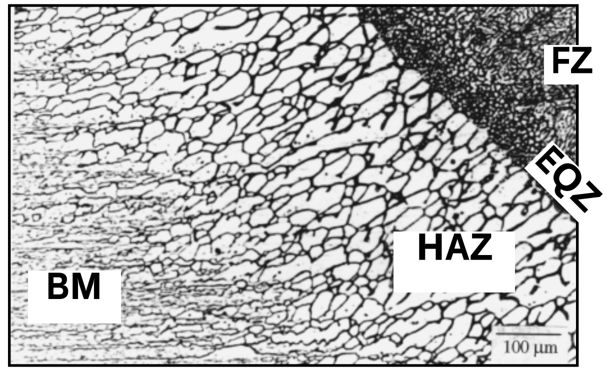

Fig. 6 — Middle left side of 1-g weld, 50X. Left to right: BM/HAZ/EQZ/FZ.

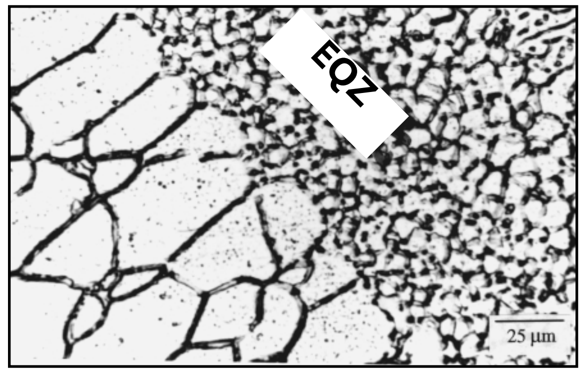

Fig. 7 — Middle left side of 1-g weld, 200X. Left to right: HAZ/EQZ/FZ.

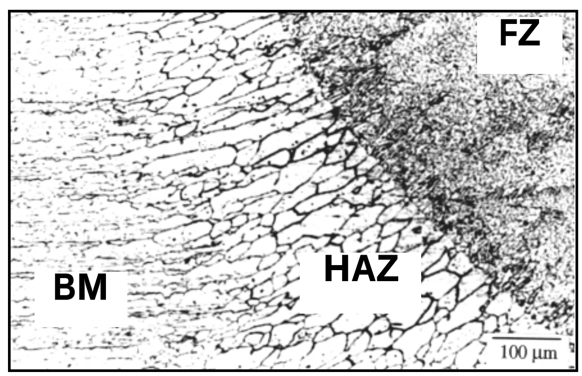

Fig. 8 — Top left side of 5-g weld, 50X. Left to right: BM/HAZ/FZ.

patibility of these alloys because liquid hydrogen and liquid oxygen make up the fuel/oxidizer combination of choice. These tanks are most often fabricated by welding because the propellants are contained under pressure (Ref. 1).

Weld defects are a particular concern in Al-Li alloys, particularly weld metal porosity. Weld metal porosity can form in Al alloys when monatomic hydrogen is partitioned interdendritically during solidification. A sufficient amount of hydrogen must be partitioned so that the interdendritic liquid becomes super saturated, thus increasing the drive for pore nucleation. Lithium-containing aluminum alloys exhibit a higher than normal propensity for weld metal porosity.

With regards to microstructure, the high strength of Al-Li weld metal is due to a combination of fine grain size and precipitate formation. This tendency toward fine-grained weld metal microstructure has been noted elsewhere (Ref. 2). Constitutional under-cooling by lithium has been ruled out as a possible cause. The tensile fracture of Alloy 2094 weldments has been found to be intergranular, associated with a band of fine grains located along the weld interface (Ref. 2). Based on phase equilibrium, two eutectic constituents are likely present in Al-Cu-Li weld metal: θ (Al_2Cu) and T_B ($Al_{15}Cu_8Li_2$) (Ref. 2). Weld metal precipitates δ′ and ß‘ (Al_3Zr) have been identified in Alloy 2090 in the as-welded condition, and plate-like precipitates, believed to be T_1 (Al_2CuLi), have been observed upon aging (Refs. 2, 12).

A recent study by Gutierrez and Lippold (Ref. 4) proposed a mechanism for the formation of an equiaxed zone (EQZ) of fine grains located along the weld interface between the fusion zone and heat-affected/partially melted zone (HAZ/PMZ). In the study, it was concluded that (among other things) 1) the nondendritic fusion boundary EQZ in Al-Cu-Li alloys is not the result of a recrystallization mechanism in the PMZ, and 2) Li and Zr are thought to be the most important elements affecting the formation of the EQZ. It was also proposed that the fusion boundary EQZ forms via a solidification mechanism in a narrow temperature region adjacent to the fusion boundary by a heterogeneous nucleation mechanism aided by Al_3Zr and $Al_3(Li, Zr)$ precipitates.

According to their study, the mechanism involved includes Li and Zr as the primary elements affecting the formation of the EQZ, whereby 1) Zr forms metastable, coherent Al_3Zr precipitates that act as effective heterogeneous nucleation sites; 2) Li combines with Al_3Zr to produce a higher volume fraction of $Al_3(Li_x, Zr_{x-1})$, thereby increasing the amount of nuclei in the unmixed zone (UMZ); and 3) the Li improves the wetting behavior at the precipitate/liquid interface by reducing the interfacial surface energy, therefore increasing the effectiveness of the nucleation process. It is these precipitates, present during the thermomechanical processing of the wrought material, that are believed to serve as nucleation sites for the nondendritic equiaxed grains (Ref. 4).

Furthermore, it was proposed that in the narrow liquid boundary adjacent to the fusion boundary, the thermal and fluid flow conditions are insufficient to allow these precipitates to undergo complete dissolution in the hotter weld pool. Additionally, the limited mixing in the UMZ is thought to result in a stagnant boundary layer that would facilitate the nucleation of small nondendritic equiaxed grains. With this in mind, the

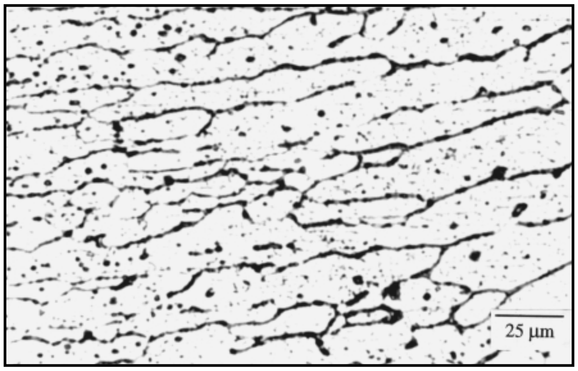

Fig. 9 — Top left side of 5-g weld, 200X. Left to right: BM/HAZ.

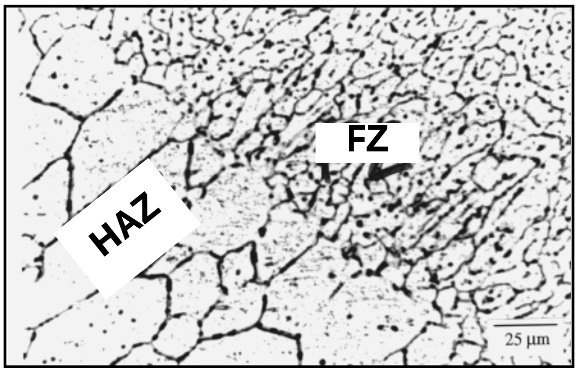

Fig. 10 — Top left side of 5-g weld, 200X. Left to right: HAZ/FZ.

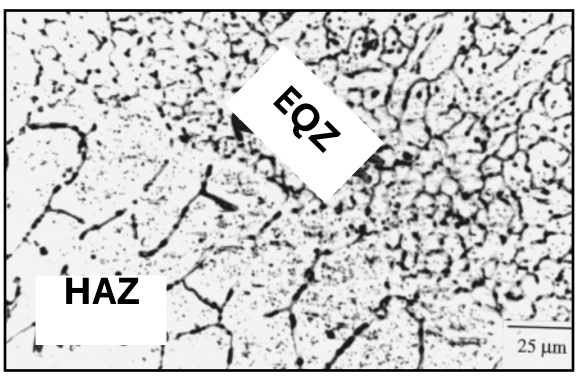

Fig. 11 — Middle left side of 5-g weld, 200X. Left to right: HAZ/EQZ/FZ.

effects of stirring the molten metal were found to effectively eliminate the EQZ by eliminating the stagnant boundary layer where nondendritic equiaxed grains nucleate.

With the Gutierrez and Lippold study in mind, it is also well known that the fluid flow and heat transfer in the melt control the resulting weld geometry, solidification morphology and mode, as well as the compositional homogeneity in the fusion zone. Buoyancy and the temperature dependence of the surface tension have been found to have significant effects on the fluid flow in Al welds (Ref. 13). Therefore, it is apparent convective flow in the weld pool and surfactants can control the presence, and possibly the existence, of some common weld defects. In this case, the defect is the formation of the EQZ. It is due primarily to buoyancy's direct relationship with gravity that the weldability of materials in various gravitational environments, both high and low, needs to be investigated.

In an effort to determine the effect of enhanced convection on aforementioned phenomena and eliminate the formation of an EQZ, welds at three different g-levels (1 g = 9.8 m/s^2) were analyzed. Comparing the resultant microstructures to each other and the accepted findings represents the bulk of the analysis presented here. Furthermore, the possible qualitative verification of the Gutierrez and Lippold study from test results became a priority.

Table 1 — Spot GTAW Parameters for 1, 5 and 10 g Using MGRWS

Welding process	GTA, DCEN
Current	125 A
Electrode type and tip	W-2%ThO_2 and 90 deg
Electrode extension	0.124 in. (3.1 mm)
Gas nozzle	0.5 in. (12.5 mm) diameter
Arc length	0.08 in. (2 mm)
Shielding gas	75% argon, 25% helium
Shielding gas flow rate	30 ft^3/h (225 cm^3/s)
Post-shield flow	30 s
Weld type	Spot (stationary) weld
Arc time	30 ± 1 s
Base metal dimensions	25.4 × 25.4 × 7.3 mm
No insulation under specimen	

Experimental Procedure

The multigravity research welding system (MGRWS) was used to quantify the effect of enhanced convection on microstructure of Al-Cu-Li welds.

Material Selection

The material under investigation during multigravity welding conditions was 2195-T8 alloy, a member of the Weldalite 049 family of Al-Li alloys. This alloy contains nominally, in weight percent, 1.0% Li, 4.0% Cu, 0.4% Mg, 0.14% Zr and 0.4% Ag. This composition was partially chosen to ensure adequate weldability of the alloy. This alloy was obtained in plate form of 7.5-mm thickness.

Welding Apparatus and Process

In order to investigate the effect of enhanced convection on the microstructure of the fusion zone (FZ), the equiaxed zone (EQZ) and the heat-affected zone (HAZ), the multigravity research welding system (MGRWS) was used for the experimentation — Fig. 1. The MGRWS has a 3.3-ft (1-m) arm length and can rotate more than 100 rpm, producing a net acceleration of greater than 16 g (1 g = 9.8 m/s^2). The MGRWS rotating is shown in Fig. 2. Note the welding box has swung outward. This hinged welding box maintains a perpendicular alignment between the net g vector and the bottom of the box, regardless of the speed of rotation, as seen in Fig. 2. The end of the centrifuge arm, which holds the welding box, is shown in Fig. 3. A small video camera is attached to the welding box and is connected to an external monitor for observing the arc initiation, propagation and termination while the centrifuge is rotating — Fig. 4. The MGRWS is capable of investigating both the GTA and GMA welding processes by simply switching power supplies and torches.

The GTA welding process was implemented to create a spot, bead-on-plate weld. Welding parameters, which were held constant for all tests except gravity level, are illustrated in Table 1. The maximum flow rate possible of 30 ft^3/h of the shielding gas was used to prevent the exposed high-temperature fusion zone from oxidizing. The 30-s arc time was chosen to provide sufficient weld pool size and was kept the same for different g levels (1 g, 5 g and 10 g).

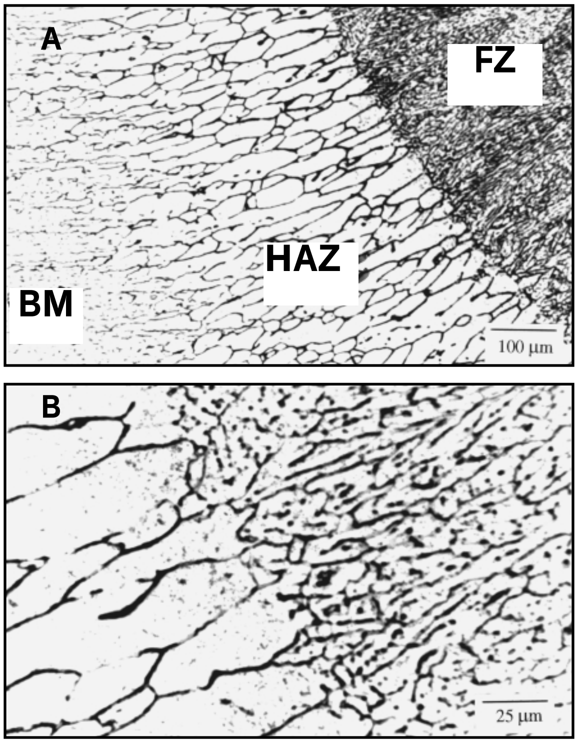

Fig. 12 — Middle left side of 10-g weld. Left to right: HAZ/FZ. A — 100X; B — 200X.

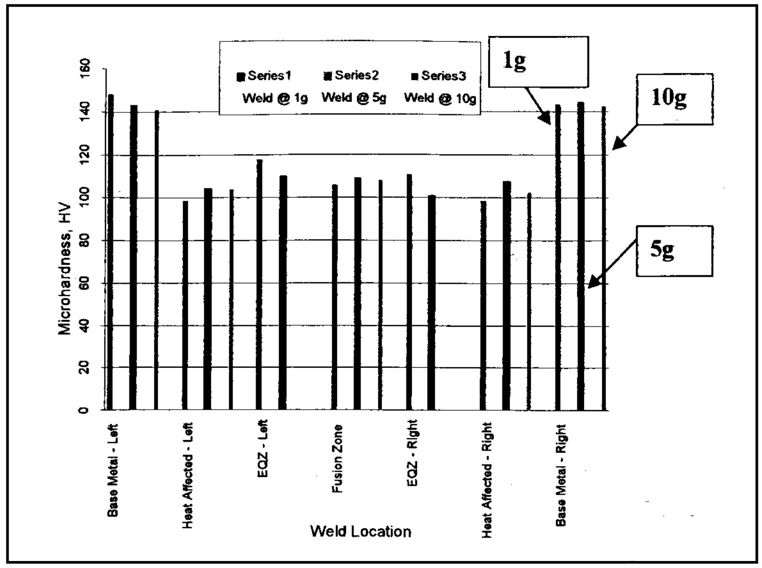

Fig. 13 — Vickers hardness vs. weld location of 1-, 5-, and 10-g welds.

Microstructural Characterization

The microstructural analysis of the three welds (1 g, 5 g and 10 g) was accomplished using optical microscopy. An Olympus microscope with a Nikon MF-19 camera attachment was implemented for optical microscopy. Micrographs of the base metal (BM), the heat-affected zone (HAZ), the equiaxed zone (EQZ) and the fusion zone (FZ) were taken at various magnifications.

Results

Microstructural Analysis

Any effort to postulate the effects of enhanced convection on fluid flow, heat and transfer, and their impact on solidification morphology, as well as the compositional homogeneity in the fusion zone (FZ), must first begin with a thorough analysis of the microstructure of the FZ and the HAZ in question. Nomenclature for various weld regions to be referred to throughout this paper is illustrated in Fig. 5.

Figure 6 is a micrograph of a weld performed at 1 g showing, from left to right, the BM, HAZ, EQZ and FZ. The BM to the far left is characteristic of a cold-worked material with a small grain size. Moving from the far left to the right within the BM, grains begin to enlarge and elongate out of the base metal as a result of grain growth supported by the heat input from the welding process. Grain boundaries appear in the middle of very large grains within the heat-affected zone/partially melted zone (HAZ/PMZ) seen in Fig. 6. This is consistent throughout the HAZ and is not believed to be a lack of etching. Grain boundary liquation is also prevalent in this region. Moving farther to the right in Fig. 6, the EQZ is located between the HAZ/PMZ to its left and the cellular dendritic structure of the FZ to its right. Figure 7 is a higher magnification of the HAZ/PMZ, EQZ and FZ regions, further emphasizing the large variance in microstructural morphology.

Figure 8 is a photomicrograph of, from left to right, the base metal (BM), the heat-affected zone (HAZ) and the fusion zone (FZ) on the top left side of a weld performed at 5-g acceleration. Moving from the far left to the right within the BM, grains begin to enlarge and elongate out of the BM as a result of grain growth supported by the heat input from the welding process. This transition is illustrated at higher magnification in the photomicrograph of Fig. 9. Grain boundaries appear to terminate in the middle of very large grains within the HAZ/PMZ. This is consistent throughout the HAZ and is not believed to be a lack of etching. Grain boundary liquation is also prevalent in this region. Moving farther to the right in Fig. 10 taken at higher magnification, the lack of an EQZ is readily apparent. The EQZ, however, reappears in micrographs of the fusion boundary region located midway down the depth of the weld as seen in Fig. 11.

The microstructure of a 10-g weld is represented by Fig. 12. Grain boundaries appear to terminate in the middle of very large grains within the HAZ/PMZ seen in Fig. 12, which is consistent with 1- and 5-g welds. Grain boundary liquation is also prevalent in this region, and the lack of an EQZ is readily apparent. EQZ formation did not occur at any location within the 10-g weld.

Hardness Measurements

Microhardness measurements of the various weld regions were performed using a Vickers diamond indenter. Hardness was measured under 40x objective and an applied load of 300 grams. Measurements were taken along a line at half the depth of the fusion zone across the entire weld region at an interval of four times the indenter's size to avoid the effects of localized strain hardening in the vicinity of the indentation. Figure 13 depicts the variance in hardness across the weld region from left to right of the base metal (BM), the heat-affected zone (HAZ), the equiaxed zone (EQZ) and the fusion zone (FZ) of 1-, 5- and 10-g welds. Values depicted in Fig. 13 are an average of five measurements per region. Because of the changing width in the EQZ, only three measurements were able to be taken per side. EQZ indentations that traversed either the HAZ or FZ were not included in the final average.

A noticeable decrease in hardness is present when moving from left to right, BM to the HAZ. Hardness then remains relatively constant moving to the right across the entire weld region with an increase in hardness occurring when emerging out of the right HAZ to the right BM.

Discussion

The gradual disappearance of the prominent EQZ found at 1 g from the fusion boundary when welding at 5 g, and its complete disappearance at 10 g, is believed to be due to enhanced convection and mixing in the fusion zone. The centrifuge's (MGRWS) generation of the high buoyancy-driven flow environment causing altered thermal and fluid flow characteristics in the weld pool is thought to eliminate the stagnant boundary layer in the unmixed zone at the fusion boundary. It is in the stagnant boundary layer within the unmixed zone where heterogeneous nucleation sites of the equiaxed grains are thought to exist as proposed by Gutierrez and Lippold (Ref. 4).

It is believed that the heterogeneous nucleation mechanism aided by Al_3Zr and $Al_3(Li, Zr)$ precipitates as was proposed (Ref. 4) is prevented by the complete dissolution of these precipitates as they are swept into the hotter weld pool. At high gravity, the stagnant boundary layer where these precipitates are found is nonexistent. Hence, the high g environment generated by the centrifuge effectively eliminates the environment suitable for the nucleation of equiaxed grains. As a result, an EQZ does not form.

The hardness of the weld regions was found to decrease from the BM to the HAZ and remained constant across the HAZ and the FZ. This was expected because of the effect of heat input on the original microstructure, reduction of dislocation density and residual stresses produced during the thermo-mechanical processing of the alloy. Hardness was not found to vary considerably from 1 to 5 to 10 g.

The MGRWS may not at the present time be of direct practical value to industry, but it is a very useful experimental tool for the researchers to gain better understanding of the physics of arc welding, the interaction of the convective forces and their role in the weldability of materials

Conclusion

The absence of an EQZ in the 10-g weldment is a significant finding due to prior observations of intergranular tensile fracture along a band of fine grains along the weld interface (Ref. 2). The proposed mechanism for heterogeneous nucleation (Ref. 4) has been qualitatively verified by results found in this study. Of particular importance are the effects of elevated gravity levels, which rid the fusion boundary of the stagnant boundary layer in the unmixed zone. The altered thermal and fluid flow properties generated by the centrifuge effectively eliminates the nucleation site of equiaxed grains by promoting rapid mixing throughout the weld pool and dissolution of precipitates believed to aid in the process.

References

1. ASM *Metals Handbook*, 10th Edition, Vol. 2.

2. ASM *Metals Handbook*, 10th Edition, Vol. 6.

3. Srivatsan, T. S., and Sudarshan, T. S. 1991. Welding of lightweight aluminum-lithium alloys. *Welding Journal* 70(7): 173-s to 184-s.

4. Gutierrez, A., and Lippold, J. C. 1998. A proposed mechanism for equiaxed grain formation along the fusion boundary in aluminum-copper-lithium alloys. *Welding Journal* 77(3): 123-s to 132-s.

5. Starke, E. A., Jr., Sanders, T. H., Jr., and Palmer, I. G. 1981. New approaches to alloy development in the Al-Li system. *J. Met.*, p. 24–33.

6. Sankaran, K. K., and Grant, N. J. 1981. Structure and properties of splat quenched 2024 aluminum alloy containing additions. *Aluminum-Lithium Alloys*. The Metallurgical Society of AIME, pp. 205–227.

7. Noble, B., and Thompson, G. E.1971. *Met. Sci. J.* 5: 114.

8. Williams, D. B., and Edington, J. W. 1974. *Met. Sci. J.* 9: 529.

9. Sanders, T. H., Jr. 1980. *Mater. Sci. Eng.* 43: 247.

10. Jha, S. C., Mahalingam, K., and Sanders, T. H., Jr. 1986. Analytical models to predict the microstructure of binary Al-Li alloys. E. A. Starke and T. H. Sanders, Jr., eds., *Aluminum Alloys and Their Physical and Mechanical Properties II,* Engineering, Materials Advisory Services Ltd.

11. Sanders, T. H., Jr., Ludwiczak, E. A., and Sawtell, R. R. 1989. *Mat. Sci Eng.* 43: 247–260.

12. Kramer, L. S., Heubaum, F. H., and Pickens, J. R. Aluminum-lithium alloys. T. H. Sanders, Jr., and E. A. Starke, Jr., eds., *Proc. 5th Int. Al-Li Conference*, Birmingham, U.K., Materials and Component Engineering Publications, Ltd.

13. Domey, J., Aidun, D. K., Ahmadi G., Regel L., and Wilcox W. R. 1995. Numerical simulation of the effect of gravity on weld pool shape. *Welding Journal* 74(8): 263-s.